

# An Approach of Abnormal Vasculature Detection on the Optic disc

J.Sweetline Arputham

**Abstract—** Proliferative Diabetic Retinopathy is the cause of blindness for the person affected with diabetes mellitus. The onset of Proliferative Diabetic Retinopathy is signaled by the appearance of abnormal retinal blood vessels on the retina and on the optic disc. The appearance of new abnormal blood vessel is known as Neovascularization. Neovascularization on the optic disc has the worst prognosis. This paper proposes a method to detect the abnormal retinal blood vessels on the optic disc. First, the optic disc is segmented by Chan Vese active contour model. Then, vessels in the retinal images are extracted by means of Ridge Strength Measurement and Watershed lines. Fifteen features associated with the shape and position of the vessels were calculated. Based on the features extracted, each segmented blood vessel is classified as normal and abnormal by using Support Vector Machine Classifier. The obtained sensitivity and specificity will be useful to reduce the workload of an ophthalmologist.

**Index Terms—** Active Contour Model, Support Vector Machine, Tortuosity measure, Vasculature, Watershed Transformation .

## I. INTRODUCTION

Diabetic retinopathy (DR) is a disease occurring in diabetes patient, which causes progressive damage to the retina of the eye. DR is the result of damage to the tiny blood vessels that nourishes the retina. They leak blood and other fluids and cause swelling of retinal tissue and clouding of vision. If left untreated, diabetic retinopathy can cause blindness. Proliferative diabetic retinopathy (PDR) mainly occurs when many of the blood vessels in the retina close, preventing enough blood flow. In an attempt to supply blood to the area where the original vessels closed, the retina responds by growing new blood vessels. These new blood vessels are usually more convoluted, twisted and prone to leak blood. This is called neovascularization. These new blood vessels are abnormal and do not supply the retina with proper blood flow. The new vessels are also accompanied by scar tissue that may cause the retina to wrinkle or detach. New vessels are classified according to their position as new vessels on the optic disc and new vessels elsewhere. New blood vessels have a narrower calibre, more tortuous and are convoluted than normal vessels. The development of the new

vessels can be inhibited by early diagnosis and treatment. here are three major treatments for diabetic retinopathy, which are very effective in reducing vision loss. These three treatments are laser surgery, injection of triamcinolone into the eye, and vitrectomy.

A number of investigations were made regarding the automatic detection of microaneurysms or haemorrhages and exudates. Little work has been done to detect vessel abnormalities such as venous beading and vessel characteristics to predict the presence of proliferative disease. J.H.Hipwell et.al proposes an automatic approach to detect diabetic retinopathy in digital red-free images that uses an algorithm that enhances small round features [2]. T. Walter et.al, proposed the method for the automatic detection of microaneurysms by diameter closing and an automatic threshold scheme [3]. T. Walter et.al, proposed a method that detect exudates using their high grey level variation, and their contours are determined by means of morphological reconstruction techniques, the optic disc is detected by means of morphological filtering techniques and the watershed transformation [4]. Osareh et.al, proposed a method to identify exudates using fuzzy C-means clustering following some key preprocessing steps. To classify the segmented regions into exudates and non-exudates, an artificial neural network classifier was used [5]. Ching-Wen Yang, present a computer-aided diagnostic system to automatically detect venous beading of blood vessels. It comprises of two modules, referred to as the blood vessel extraction module (BVEM) and the venous beading detection module (VBDM). The former uses a bell-shaped Gaussian kernel to extract blood vessels while the latter applies a neural network to detect venous beading among the extracted blood vessels for diagnosis [6]. Herbert F. Jelinek, proposed a method to detect proliferative retinopathy, Fluorescein-labeled retinal blood vessels were automatically segmented using the Gabor wavelet transform and classified using traditional features such as area, perimeter [7].

This paper proposes a way to detect the Proliferative Diabetic Retinopathy on the Optic Disc. Since this work focuses on the optic disc, first the segmentation of the optic disc is done by Chan-Vese Active Contour Model.

*Manuscript received June, 2014.*

J.Sweetline Arputham, Department of Computer Science and Engineering, Dr.G.U.Pope College of Engineering, Thoothukudi, India+919965397992

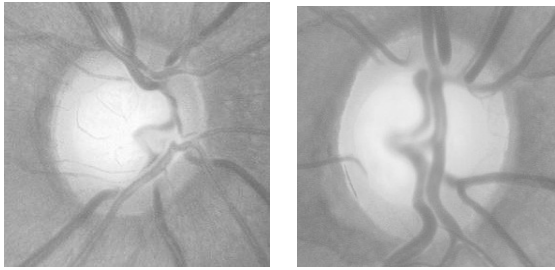


Fig -1: Sample Normal Image

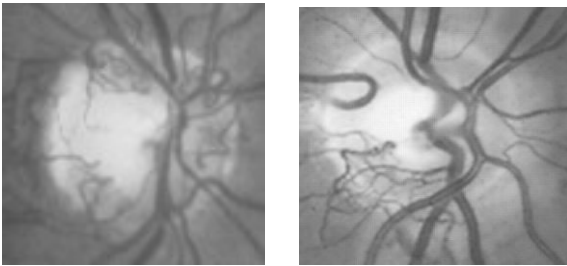


Fig -2: Sample Abormal Neovascularization Image

II. METHOD

A. Optic Disc Segmentation

Since, the optic disc is the entry point for the blood vessels, the damage or the growth of the new blood vessels on the optic disc will result in the severe vision loss. There are number of methods have been proposed on the segmentation of the optic disc. Initial attempts have been made with shape-based template matching in which OD is modeled as a circular [8][9] or elliptical [10] object. This matching is performed on an edge map extracted from the underlying image. This approach suffers due to vessel edges present in and around the OD region. Chan-Vese active contour method is used to detect the optic disc [11][12]. To detect the optic disc in some pathological condition, the following is made. First the red color plane of the image is used to detect the optic disc in the retinal image. Gaussian filter is used with three different sigma values such as 2,  $\sqrt{2}$ ,  $2\sqrt{2}$  are calculated and fused. Next, the fused image is used to calculate the Grey value descriptors by,

$$L(c, \sigma, \tau) = L_0(\sigma, \tau) + \cos\left(\frac{\pi \tau c}{\sigma}\right) e^{-\frac{c^2}{2\sigma^2}} \tag{1}$$

where,  $\tau$  is the number of cycles of the harmonic function within the Gaussian envelope of the filter, commonly used in the context of Gabor filters. The contour is initialized using the circular hough transform. The circle points are identified using estimated radius and used to initialize the active contour. This model is based on an energy minimization problem, which can be reformulated in the level set formulation, leading to an easier way to solve the problem. The minimized energy function is

$$E(h^+, h^-, C) = \int \tilde{E}x(h^+, h^-, C) dx \tag{2}$$

The above energy function can be rewritten in the Level-set formulation using the Heaviside function as

$$E(h^+, h^-, \phi) = \int \left[ \frac{1}{2} \sum_{i=1}^d \lambda_i^+ \int k(x, y) |I_i(y) - h_i^+|^2 H(\phi(y)) dy \right] dx + \int \left[ \frac{1}{2} \sum_{i=1}^d \lambda_i^- \int k(x, y) |I_i(y) - h_i^-|^2 (1-H(\phi(y))) dy \right] dx \tag{3}$$

The energy function value is minimum on the boundary.

B. Blood Vessel Segmentation

The green color plane of the image is chosen. The green color plane shows the best contrast between the vessel and the background retina. The blood vessel is segmented using Ridge strength and Watershed Transformation.

Ridge Strength

Ridges are defined as points where the image has an extrema in the direction of the largest surface curvature. The ridge strength can be calculated by the dark ridges that are formed by the vessel center lines. Ridge strength  $k$ , is given by [13]

$$k = \frac{L^2_x L_{yy} + L^2_y L_{xx} - 2L_x L_y L_{xy}}{(L^2_x + L^2_y)^{3/2}} \tag{4}$$

where,  $L$  represents the Gaussian filtered image,  $L_x$  and  $L_y$  represents the first partial derivative of  $L$  with respect to  $x$  and  $y$  and  $L_{xx}$ ,  $L_{yy}$ ,  $L_{xy}$ ,  $L_{yx}$  represents the second partial derivative of  $L_x$  and  $L_y$ . The value of the ridge strength  $k$  is positive for the vessel ridges, negative for areas between the vessels and undefined for the areas where the gradient in both  $x$  and  $y$  direction is zero.

Applying an empirically derived threshold,  $k_{thres}$  is used for the segmentation of the blood vessels. The above method produces a large number of disjoint vessels.

Watershed Transformation

Watershed Transformation is the morphological region based segmentation method based on the topology of the image[14]. The grey image forms the topographic surface. Watershed Transformation divides the image into regions based on the image grey level. The dividing lines are called the Watershed lines and the grouped regions are called the catchment basins. The grey level is inverted such that the blood vessels form the watershed lines. The inverted grey image is filtered with the Gaussian filter such that over-segmentation can be avoided. The watershed regions are calculated using Meyer’s algorithm as

1. A set of markers, pixels where the flooding shall start, are chosen.
2. The neighboring pixels of each marked area are inserted into a priority queue with a priority level corresponding to the grey level of the pixel.
3. The pixel with the highest priority level is extracted from the priority queue. If the neighbors of the extracted pixel that have already been labeled all have the same label, then the

pixel is labeled with their label. All non-marked neighbors that are not yet in the priority queue are put into the priority queue.

4. Redo step 3 until the priority queue is empty.

The Watershed Transformation produces closed regions connected by the watershed lines. To remove the non-vessel segments the mean value of 'k' along each candidate segment is calculated and candidates with mean values less than  $k_{thres}$  are discarded.

C. Feature Extraction

Features were calculated for each segment, based on characteristics human observers use to recognize abnormal vessels. The vessel origin was estimated as follows. Firstly, a median filter was applied to remove smaller vessels. Next a threshold was applied to select the darkest 20% of pixels, which were assumed to belong to the major blood vessels. The centroid of the result was taken as the approximate origin of the major vessels. The following features were calculated for each segment.

**Segment length and Direction:** The length of each blood vessel from the origin calculated in pixel.

The angle between a tangent to the segment center point and a line from its center point to the vessel origin. The feature segment direction is based on the observation that normal vessels tend to radiate from the vessel origin towards the edge of the disc, whereas the direction of new vessels is more random.

**Gradient and Gradient Variation:** The gradient magnitude of the image at each point gives the direction of the largest possible change in the intensity of the grey image. The gradient is calculated using Sobel gradient operator as

$$G = \sqrt{G_x^2 + G_y^2} \tag{5}$$

where  $G_x, G_y$  represents the convolution of original image with the kernel. The mean of the gradient is calculated.

The standard deviation of the Sobel gradient is calculated. Gradient Variation is based on the observation that the abnormal vessels have more contrast variation than the normal vessels.

**Tortuosity Measures:** The sum of the absolute changes in the tangential direction along segment path

$$T_1 = \frac{1}{n-1} \sum_{i=1}^{n-1} |\theta_{i+1} - \theta_i| \tag{6}$$

where,  $\theta_i$  is the tangential angle at the  $i^{th}$  element.

The difference in the angular extrema of the segment tangents

$$T_2 = \max_{i=1 \dots n} \{ \theta_i \} - \min_{i=1 \dots n} \{ \theta_i \} \tag{7}$$

The third tortuosity measure was the mean change in direction per pixel along the segment.

$$T_3 = \frac{1}{n} \sum_{i=1}^n k_i \tag{8}$$

where,

$$k_i = \begin{cases} 1, & \text{if } \begin{cases} \left| \frac{d^2x}{di^2}(i) \right| = 1 \text{ and } \frac{d^2y}{di^2} = 0 \\ \frac{d^2x}{di^2}(i) = 0 \text{ and } \frac{d^2y}{di^2}(i) = 1 \end{cases} \\ \sqrt{2}, & \text{if } \frac{d^2x}{di^2}(i) = 1 \text{ and } \frac{d^2y}{di^2}(i) = 1 \\ 0, & \text{otherwise} \end{cases} \tag{9}$$

where, x and y are the Cartesian coordinates.

The above three tortuosity feature is based on the observation that abnormal vessels are more twisted than the normal vessels.

**Grey Level and Grey Level Coefficient of Variation:** The normalized mean grey level

$$g_{norm} = \frac{1}{G_{max} - G_{min}} \left[ \left( \frac{1}{n} \sum_{i=1}^n g_i \right) - G_{min} \right] \tag{10}$$

where  $g_i$  is the grey level of the  $i^{th}$  segment pixel and  $G_{max}$  and  $G_{min}$  are the maximum and minimum grey level values in the original image.

The ratio of the mean and standard deviation of the segment grey level values. This Grey level Coefficient of variation is based on the observation that the abnormal vessels have greater variation of grey level than abnormal blood vessels.

**Distance from origin and Number of Segments:** The distance from the center of the segment to the vessel origin in pixel. The distance from origin feature is based on the observation that the abnormal vessels occur towards the edge of the disc.

The total number of segments following the candidate segmentation is considered as the number of segments. The abnormal vessels have more number of segments than normal vessels and so the feature number of segment is considered.

**Vessel Density and Width:** The segment surrounding the segment 'a' were determined using

$$O(a) = \{ b | s(a) \oplus D \} \cap s(b) \neq \emptyset \tag{11}$$

where,

$b \in S$  and  $b \neq a$

where S is the set of all segments and  $s(a) \oplus D$  denotes the dilation between the path of segment 'a' and structuring element D. The density was taken as the number of elements in O(a) divided by the length of the segment 'a'.

The distance from each segment point to the closest edge point is assumed to be the vessel half-width at that point. This feature vessel width is based on the observation that the abnormal vessels are normally very fragile and so the vessel width will be smaller than abnormal vessel.

**Mean Ridge Strength:** The value of k by the equation (4).

**Mean Vessel wall gradient:** The mean value of the Sobel gradient magnitude for all the vessel wall points.

D. Classification

Support Vector Machine is used as the classifier, for its good classification performance. A classification task usually involves separating data into training and testing sets. Each instance in the training set contains one target value (i.e. the class labels) and several attributes (i.e. the features or observed variables). The goal of SVM is to produce a model (based on the training data) which predicts the target values of the test data given only the test data attributes.

The training vectors are mapped into a higher dimensional space for classification. The transformation to the higher dimensional space involves the kernel function. SVM finds a hyperplane with the maximal margin in the higher dimensional space. The kernel function used to transform the original feature space to transformed feature space is the radial basis function [15][16][17].

$$K(x_i, x_j) = \exp(-\gamma \|x_i - x_j\|^2) \quad \gamma > 0 \tag{12}$$

where,  $x_i, x_j$  are the feature vectors for the two classes and  $\gamma$  is a configurable parameter.

Training

The retinal image containing the optic disc is first segmented using the Chan-Vese active contour model and the blood vessels are extracted by the Watershed transformation and fifteen features corresponding to the shape and position of the blood vessels are extracted and the features are saved. This training process comprises of training the normal and abnormal images and the features are saved separately for normal and abnormal images.

Testing

The image to be tested is given as an input and the segmentation of the optic disc is done. The blood vessels are extracted by the Watershed Transformation and fifteen features corresponding to each of the blood vessels are extracted and given as an input to the SVM classifier. Based on the training data, the test image features are classified as normal or abnormal.

III. SIMULATION RESULT

The above work is carried out with the dataset of 32 images, out of which 23 are normal images and 9 are abnormal images. The image that are actually normal image and classified as normal are called True negative, and if the same image is classified as abnormal, it is said to be false positive. The image that are actually abnormal and classified as normal are called False negative and if the same image is classified as abnormal, it is said to be True positive. The accuracy is calculated in terms of sensitivity and specificity as

$$\text{Sensitivity} = \frac{\text{No. of True Positive}}{\text{No. of True Positive} + \text{No. of False Negative}}$$

$$\text{Specificity} = \frac{\text{No. of True Negative}}{\text{No. of True Negative} + \text{No. of False Positive}}$$

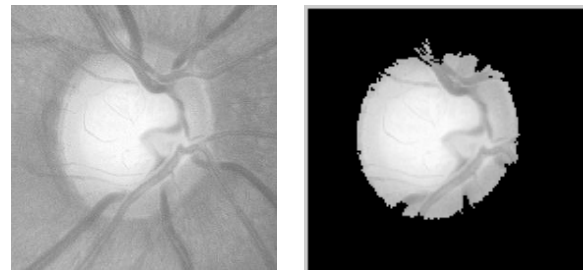


Fig -3: Segmented Optic Disc

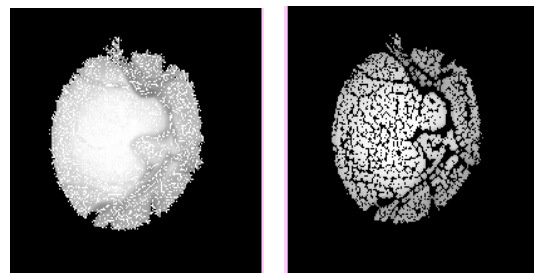


Fig -4: Segmented Blood Vessels by Ridge Strength and Watershed Transformation

The images are classified as normal or abnormal by considering five features, ten features and fifteen features. The following table shows the sensitivity and specificity obtained by considering features. The system obtained the maximum sensitivity and specificity of 84.7% and 86.1% while considering fifteen features. But, when considering five features the sensitivity and specificity obtained are 66.67% and 76.92%, while considering ten features the system attains 83.52% and 84.61% of sensitivity and specificity. The obtained accuracy is sufficient to perform the clinical role and to decrease the workload of an ophthalmologist.

Table -1: Accuracy based on Features Considered

Features \ Accuracy	5 features	10 features	15 features
Sensitivity	66.67	83.52	84.7
Specificity	76.92	84.61	86.1

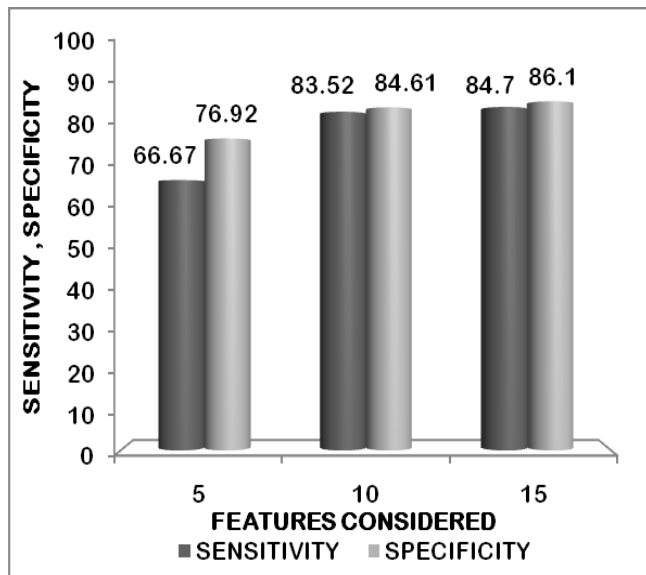


Chart -1: Graphical Representation of Accuracy

#### IV. CONCLUSION

The described method to detect the proliferative diabetic retinopathy shows the sensitivity and specificity of 84.7% and 86.1%. Compared to our previous method of detecting the disease as mentioned in [1], the system shows higher accuracy when detecting the optic disc by Chan-Vese active contour model. Since this work detects the disease only on the optic disc, further steps shall be taken to detect the new vessels on the retina. The use of other classifiers such as knn classifier and the combination of two or more classifiers may also improve the classification performance. Furthermore, the combination of the proliferative diabetic retinopathy detection system with the additional image analysis tool such as non proliferative diabetic retinopathy detection system will prevent the vision loss in the diabetic patient.

#### REFERENCES

- [1]. Keith A. Goatman, Alan D. Fleming, Sam Philip, Graeme J. Williams, John A. Olson, and Peter F. Sharp, "Detection of New Vessels on the Optic Disc Using Retinal Photographs," IEEE Trans. Med. Imag., vol. 30, no. 4, pp. 972–979, April 2011.
- [2]. J. H. Hipwell, F. Strachan, J. A. Olson, K. C. McHardy, P. F. Sharp, and J.V.Forrester, "Automated detection of microaneurysms in digital red-free photographs: A diabetic retinopathy screening tool," Diabetic Med., vol. 17, pp. 588–594, 2000.
- [3]. T. Walter, P. Massin, A. Erginay, R. Ordonez, C. Jeulin, and J. Klein, "Automatic detection of microaneurysms in color fundus images," Med. Image Anal., vol. 11, pp. 555–566, 2007.
- [4]. T. Walter, J. C. Klein, P. Massin, and A. Erginay, "A contribution of image processing to the diagnosis of diabetic retinopathy-detection of exudates in color fundus images of the human retina," IEEE Trans. Med. Imag., vol. 21, no. 10, pp. 1236–1243, Oct. 2002.
- [5]. A. Osareh, M. Mirmehdi, B. Thomas, and R. Markham, "Automated identification of diabetic retinal exudates in digital colour images," Br J. Ophthalmol., vol. , pp. 1220–1223, 2003.
- [6]. C.W.Yang, D.J.Ma, S.C.Chao, C. M. Wang, C. H. Wen, C. S. Lo, P. C. Chung, and C. I. Chang, "Computer-aided diagnostic detection system of venous beading in retinal images," Opt. Eng., vol. 39, pp. 1293–1303, 1995.
- [7]. H. F. Jelinek, M. J. Cree, J. J. G. Leandro, J. V. B. Soares, R. M. C. Jr and A. Luckie, "Automated segmentation of retinal blood vessels and identification of proliferative diabetic retinopathy," J. Opt. Soc. Am. A, vol. 24, pp. 1448–1456, 2007.

- [8]. M. Lalonde, M. Beaulieu, and L. Gagnon, "Fast and robust optic disc detection using pyramidal decomposition and hausdorff-based template matching," IEEE Trans. Med. Imag., vol. 20, no. 11, pp. 1193–1200, Nov. 2001.
- [9]. R. Chrastek, M. Wolf, K. Donath, G. Michelson, and H. Niemann, "disc segmentation in retinal images," in Proc. BVM, 2002, pp. 263–266.
- [10]. R. A. Abdel-Ghaffar and T. Morris, "Progress towards automated detection and characterization of the optic disc in glaucoma and diabetic retinopathy," Informatics Health Social Care, vol. 32, no. 1, pp. 19–25, 2007.
- [11]. T. Chan and L. Vese, "Active contours without edges," IEEE Trans. Image Process., vol. 10, no. 2, pp. 266–277, Feb., 2001.
- [12]. Gopal Datt Joshi, Jayanthi Sivaswamy and S. R. Krishnadas, "Optic Disk and Cup Segmentation From Monocular Color Retinal Images for Glaucoma Assessment", IEEE Trans. Med. Imag., vol. 30, no. 6, pp. 1192–1205, Mar. 2011.
- [13]. T. Lindeberg, "Scale-space theory: A basic tool for analysing structures at different scales," J. Appl. Stat., vol. 21, pp. 225–270, 1994.
- [14]. Meyer, "Topographic distance and watershed lines," Signal Process. vol. 38, pp. 113–125, 1994.
- [15]. B. E. Boser, I. Guyon, and V. Vapnik, "A training algorithm for optimal margin classifiers," in Proc. 5th Annu. Workshop Computat. Learn. Theory, 1992, pp. 144–152.
- [16]. V. N. Vapnik, *Statistical Learning Theory*. New York: Wiley, 1998.
- [17]. T. F. Wu, C. J. Lin, and R. C. Weng, "Probability estimates for multiclass classification by pairwise coupling," J. Mach. Learn. Res., vol. 5, pp. 975–1005, 2004.

**Sweetline Arputham** was born in India in 1988. She received the B.E and M.E degree in Computer Science and Engineering from Anna University in 2010 and 2012 respectively. She is working as an Assistant Professor in Dr.G.U.Pope College of Engineering, TamilNadu, India.